Latrophilin2 is involved in neural crest cell migration and placode patterning in *Xenopus laevis*

NATSUMI YOKOTE[#,1,2], MARIANNA Y. SUZUKI-KOSAKA[#,1,2], TATSUO MICHIUE[3],
TAKAHIKO HARA[*,1,2] and KOSUKE TANEGASHIMA[*,1]

[1]Stem Cell Project, Tokyo Metropolitan Institute of Medical Science, Setagaya-ku,
[2]Graduate School of Medical and Dental Sciences, Tokyo Medical and Dental University, Bunkyo-ku and
[3]Department of Life Sciences, University of Tokyo, Meguro-ku, Tokyo, Japan

ABSTRACT Latrophilin2 (Lphn2) is an adhesion-class of G protein-coupled receptor with an unknown function in development. Here, we show that *Xenopus laevis lphn2* (*Xlphn2*) is involved in the migration and differentiation of neural crest (NC) cells and placode patterning in *Xenopus laevis* embryos. Although *Xlphn2* mRNA was detected throughout embryogenesis, it was expressed more abundantly in the placode region. Morpholino antisense oligonucleotide-mediated knockdown of *Xlphn2* caused abnormal migration of NC cells, irregular epibranchial placode segmentation, and defective cartilage formation. Transplantation of fluorescently-labeled NC regions of wild-type embryos into *Xlphn2* morpholino-injected embryos reproduced the defective NC cell migration, indicating that *Xlphn2* regulates the migration of NC cells in a non-cell autonomous manner. Our results suggest that *Xlphn2* is essential for placode patterning and as a guidance molecule for NC cells.

KEY WORDS: *latrophilin, neural crest, placode*

Introduction

Neural crest (NC) cells are multipotent stem cells that give rise to a variety of cell lineages including melanocytes, craniofacial cartilage and bone, smooth muscle, and peripheral and enteric neurons and glia (Huang and Saint-Jeannet, 2004). Cranial NC cells are highly motile and migrate along branchial arches (Kulesa *et al.*, 2010). During NC cell migration, placode precursors chemoattract NC cells that locomote collectively (Steventon *et al.*, 2014; Theveneau *et al.*, 2010). Conversely, repulsion of placode precursors by NC cells, which is similar to contact inhibition, prevents the intermingling of NC cells and placode-derived cells (Steventon *et al.*, 2014; Theveneau *et al.*, 2013). The interaction between NC cells and placodal cells specifies a subdivision of NC cells in the branchial arches (Steventon *et al.*, 2014). Impairment of NC cell migration is a causative factor for craniofacial birth defects including cleft lip, cleft palate, and the malformation of facial structures (Marcucio *et al.*, 2015). Understanding the mechanism of NC cell migration is important for understanding the etiology of these craniofacial diseases.

The adhesion-class of G protein-coupled receptors, which includes the latrophilin family of proteins (LPHN1, LPHN2, and LPHN3), have a C-terminal seven-transmembrane domain and a large N-terminal extracellular domain that are implicated in cell-cell and extracellular matrix interactions (Langenhan *et al.*, 2013). Human LPHN1 is involved in evoked exocytosis of neurotransmitters induced by spider venom (Capogna *et al.*, 2003; Deak *et al.*, 2009). As endogenous ligands for LPHN1 and LPHN3, Lasso (a splice variant of teneurin-2) and fibronectin leucine-rich repeat transmembrane proteins were identified, respectively (Silva *et al.*, 2011; O'Sullivan *et al.*, 2012). It is of note that an *LPHN3* variant has been linked statistically with the onset of attention-deficit/hyperactivity disorder (Arcos-Burgos *et al.*, 2010). Knockout of *Lphn2* in the hippocampal CA1 region of mice affected spatial memory retention, suggesting that *Lphn2* regulates synaptic function (Anderson *et al.*, 2017).

Abbreviations used in this paper: Lphn, latrophilin; NC, neural crest.

*Address correspondence to: Kosuke Tanegashima. Stem Cell Project, Tokyo Metropolitan Institute of Medical Science, 2-1-6 Kamikitazawa, Setagaya-ku, Tokyo 156-8506, Japan. Tel: +81-3-5316-3130. Fax: +81-3-5316-3226. E-mail: tanegashima-ks@igakuken.or.jp - ⓘD https://orcid.org/0000-0001-8733-8538 or
Takahiko Hara. Stem Cell Project, Tokyo Metropolitan Institute of Medical Science, 2-1-6 Kamikitazawa, Setagaya-ku, Tokyo 156-8506, Japan. Tel: +81-3-5316-3130. Fax: +81-3-5316-3226. E-mail: hara-tk@igakuken.or.jp - ⓘD https://orcid.org/0000-0002-6565-0720

#Note: These authors contributed equally to this study.

According to the European Mouse Mutant Archive (https://www.infrafrontier.eu/), the mouse *Lphn2* knockout is embryonic lethal around E15.5 (EMMA ID: EM:02294). However, the developmental functions of *Lphn2* remain to be clarified. Here, we show that the frog ortholog of *Lphn2* (*Xlphn2*) is involved in NC cell migration and differentiation.

Results

Identification and expression of Xlphn2 *gene*

Three latrophilin-family genes have been identified in mouse and human. We searched for frog orthologs of LPHN1-3 in the *Xenopus laevis* genome database and identified *Xlphn1* on chromosome 3S/L, *Xlphn2* on chromosome 4S/L, and *Xlphn3* on chromosome 1S (Fig. S1). *Xlphn2* gene analysis showed that *Xlphn2* protein contains a galactose binding lectin domain, an olfactomedin-like domain, a G-protein-coupled receptor proteolytic site, and a seven transmembrane receptor domain, which are conserved among Latrophilins and are highly identical to their vertebrate orthologs (Fig. S2). The expression of *Xlphn2* mRNA was detected in the fertilized embryo to tadpole stages, whereas *Xlphn1* was expressed after stage 25 (Fig. 1A). The expression of *Xlphn3* was not detected until stage 35 (data not shown). Whole mount *in situ* hybridization (WISH) analysis also revealed that *Xlphn2* was expressed ubiquitously in the fertilized embryo to the early neurula stage. At stage 23, we noticed that *Xlphn2* mRNA was expressed more abundantly in placodes, neural tissue, and pronephric primodia (Fig. 1B). This locally concentrated expression of *Xlphn2* continued to stage 30 in the epibranchial placodes, pronephros, midbrain, and rhombomere region (Fig. 1C). As a negative control, sense probe for *Xlphn2* revealed no expression in this experimental setting (Fig. 1D, E).

### Xlphn2 *morphants show a reduced head structure with cartilage defects*

Based on the *Xenopus laevis* genomic DNA sequence, we designed an *Xlphn2*-specific morpholino antisense oligonucleotide (MO) to disrupt functionally two *Xlphn2* genes on chromosome 4S and 4L. This *Xlphn2* MO suppressed fluorescence produced by *enhanced green fluorescent protein* (*EGFP*) mRNA fused with the 5'UTR of *Xlphn2*, but not by that of *EGFP* alone (Fig. S3). Injection of control MO did not affect embryonic development (Fig. 2A). By contrast, the *Xlphn2* MO-injected embryos exhibited a reduced head structure, mild suppression of eye development, and a bend in the anterior-posterior axis at stage 35 (Fig. 2B). These phenotypes were reversed to normal morphology (as shown in the uninjected control) by co-injection with human *LPHN2-FLAG* mRNA (Fig. 2C, D). *In situ* hybridization using probes for the neural marker *N-CAM* showed that the expression of *N-CAM* was not affected by *Xlphn2* MO except for slightly diminished staining in the eye region (Fig. 2 E,F). Quantitative reverse-transcription PCR (qRT-PCR) revealed that *N-CAM* expression was unchanged at stage 30 whereas the expression of a lens marker, *β-crystallin*, was suppressed (Fig. S4). Since lens structure was derived from placode (Schlosser, 2006), the injection of *Xlphn2* MO may induce the defects in the lens placode. In NC-derived tissues, pigmented cells were reduced slightly in developing *Xlphn2* MO-injected embryos until stage 40 (Fig. 2 G,H). Alcian blue staining also indicated that the cranial cartilage derived from NC was diminished at tadpole stage in the *Xlphn2* MO-injected embryo compared to the control MO-injected embryo (Fig. 2 I,J). Especially, branchial cartilage was more severely affected than meckel's or ceratohyal cartilage (Fig. 2 I,J).

Xlphn2 *is required for the migration and proper distribution of neural crest cells*

We examined the expression of NC markers in *Xlphn2* MO-injected embryos. The expression pattern of the pan-NC marker *Xtwist* (Hopwood *et al.*, 1989, Lander *et al.*, 2013) was not altered at stage 15 in the *Xlphn2* morphant, suggesting that *Xlphn2* is not required for the induction of NC cells (Fig. S 5 A,B). *Xtwist* staining also revealed that the migration of NC cells was reduced in the *Xlphn2* MO-injected embryos at stage 23 compared with the control MO-injected embryos (Fig. 3 A,B). However, by stage 30, *Xtwist*-positive NC cells had migrated into branchial arches in both control and *Xlphn2* MO-injected embryos (Fig. 3 C,D). In the control MO-injected embryo, four *Xtwist*-positive segments appeared along branchial arches (Fig. 3C, arrowhead), consistent
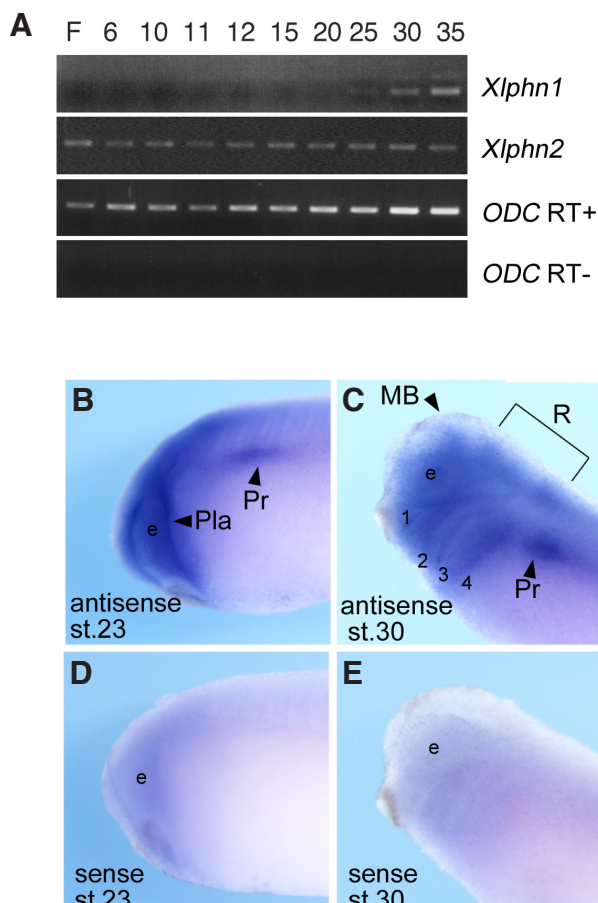

Fig. 1. Temporal and spatial expression of *Xlphn2*. (A) *RT-PCR analysis was performed at various developmental stages. Lanes indicate stages according to Nieuwkoop and Faber (1956), except for F, which represents fertilized embryo.* **(B-E)** *Whole mount* in situ *hybridization reveals the spatial expression of* Xlphn2 *(B,C) Lateral view of stage 23 (B) or stage 30 (C) embryos stained with antisense probe of* Xlphn2. *(D,E) Lateral view of stage 23 (D) or stage 30 (E) embryos stained with sense probe of* Xlphn2. *Pla, preplacode; Pr, pronephros; e, eyes; MB, midbrain; R, rhombomeres; 1-4, epibranchial placode 1-4.*
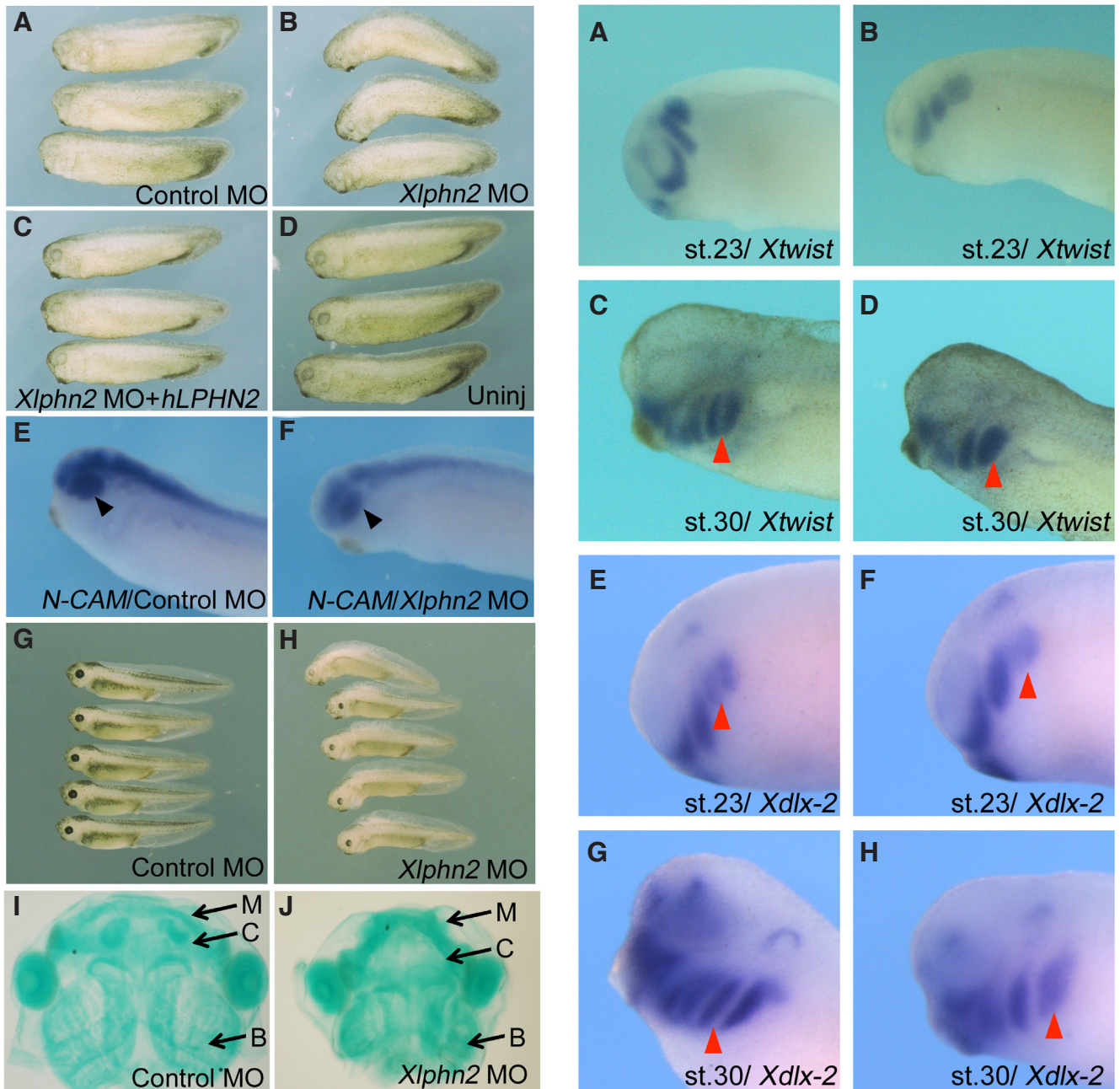
Fig. 2 (left). Phenotypes of *Xlphn2* MO-injected embryos. (A-F) *Morphology of morpholino antisense oligonucleotide (MO)-injected embryos at stage 35* **(A-D)** *and stage 40* **(E,F)**. *Forty nanograms of control MO* **(A,E)**, *40 ng of Xlphn2 MO* **(B,F)**, *or 40 ng of Xlphn2 MO with 1 ng of human LPHN2-FLAG mRNA* **(C)** *was injected into the animal pole of 2-cell stage embryos. The embryos were grown until desired stages to assess morphology. Uninjected sibling control is shown in* **(D)**. **(A)** *n=52, normal morphology 100%;* **(B)** *n=57, reduced head structure with bent axis formation 95%;* **(C)** *n=20, normal morphology 85%;* **(D)** *n=84, normal morphology 100%.* **(E,F)** *N-CAM staining of control MO* **(E)**, *or Xlphn2 MO* **(F)***-injected stage 35 embryos. Black arrowheads show staining of the eye region.* **(G,H)** *Morphology of control MO* **(G)** *and Xlphn2 MO* **(H)***-injected embryos at stage 40 (n=23 each).* **(I,J)** *Alcian blue staining of control MO* **(I)**, *or Xlphn2 MO* **(J)***-injected stage 45 embryos. M, meckel's cartilage; C, ceratohyal cartilage; B, branchial cartilage.*

Fig. 3 (right). Whole mount *in situ* hybridization of neural crest genes. *Forthy ng of control MO* **(A,C,E,G)** *or Xlphn2 MO* **(B,D,F,H)** *was injected into the animal pole of 2-cell stage embryos. The embryos were grown until they reached the desired stage for WISH. Xtwist* (A-D) *and Xdlx-2* (E-H) *were used as probes for staining stage 23 (A, B, E, F) and 30 (C, D, G, H) embryos. Streams of neural crest cells in the branchial arches are indicated by red arrowheads.*
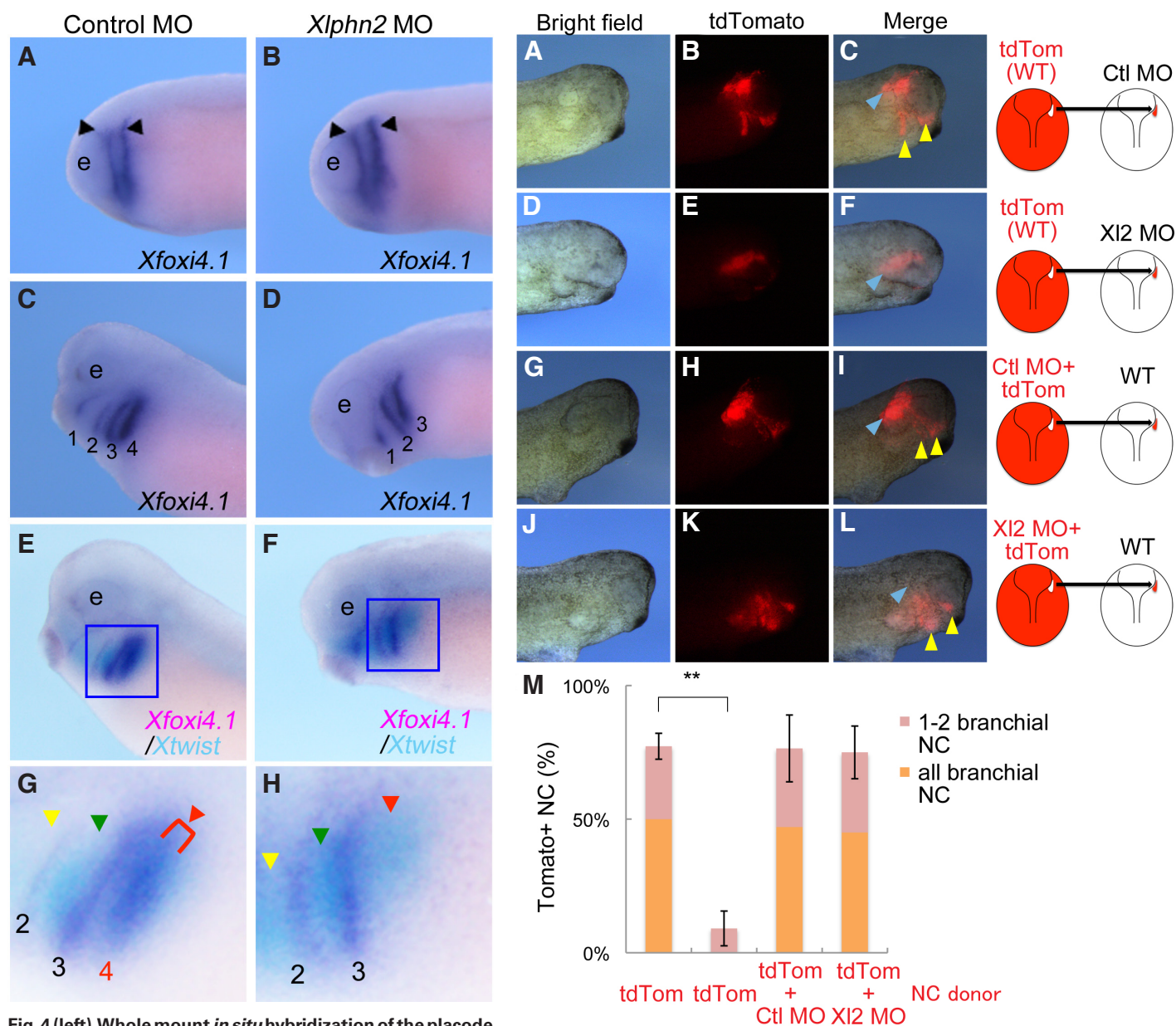
Fig. 4 (left). Whole mount *in situ* hybridization of the placode marker. *Forty ng of control MO* (A,C,E,G) *or Xlphn2 MO* (B,D,F,H) *was injected into the animal pole of 2-cell stage embryos. The embryos were grown until they reached desired stages for WISH. Stage 23 and 30 embryos were stained with* Xfoxi4.1 *as a probe (A-D).* (A,B) *Stage 23,* (C,D) *stage 30, and* (E,F) *stage 30 embryos double-stained with* Xtwist *(light blue) and* Xfoxi4.1 *(purple).* (G,H). *A magnified view of a double-stained embryo indicated as box in* (E,F) *was shown. Black arrowheads, presumtive placode region; e, eyes; 1–4, epibranchial placode 1–4; yellow arrowhead, mandibular arch neural crest cells; green arrowhead, hyoid arch neural crest cells; red arrowhead, branchial arch neural crest cells.*

Fig. 5 (right). **Neural crest (NC) cells were transplanted into stage 20 embryos, and photographed at stage 30 with fluorescent imaging. (A-F)** *tdTom-injected NC cells were transplanted into control (Ctl) MO-injected (A-C, n=22) or Xlphn2 (Xl2) MO-injected embryos (D-F, n=22).* (B,E) *tdTomato fluorescent images are shown.* (C,F) *Merged images are shown. Light blue arrowhead, unmigrated NC; yellow arrowhead, migrated NC.* (G-L) *Control (Ctl) MO+tdTom (G-I, n=11) or Xlphn2 (Xl2) MO+tdTom (J-L, n=12) -injected NC cells were transplanted into wild-type host embryos. (H, K) tdTomato fluorescent images are shown.* (I,L) *Merged images are shown. Light blue arrowhead, unmigrated NC; yellow arrowhead, migrated NC.* (M) *Statistical analysis of transplanted embryos was calculated. The percentages of migrated NCs in different experiments are shown as means with standard error. The numbers of distinct streams containing tdTom-labeled NCs were counted and added to the bar graph. Statistical analyses against samples of the control MO-injected host transplanted with tdTom-injected NC cells were performed using Fisher's exact t-test to determine statistical significance using the total number of transplanted embryos. **p< 0.01 was considered significant.*

with the results of a previous report (Lander *et al.*, 2013). In the *Xlphn2* MO-injected embryo, the third arch became wider and overlapped with the region of the fourth arch (Fig. 3D, arrowhead). qRT-PCR analysis showed that the expression levels of neural crest markers, *Xtwist* and *Xsox10*, were not affected by injection of *Xlphn2* MO (Fig. S4). Next, we examined the expression of *Xdlx-2*, which marks migratory and post-migratory craniofacial NC cells (Square *et al.*, 2015). The staining pattern of *Xdlx-2* confirmed that the third and fourth branchial arches were not separated, even at stage 23, in the *Xlphn2* MO-injected embryos compared with the control MO-injected embryos (Fig. 3 E,F, arrowhead). At stage 30, the *Xdlx-2*-positive region covered the third and fourth branchial arches in the *Xlphn2* MO-injected embryo (Fig. 3 G,H). These results suggest that *Xlphn2* regulates the migration and proper distribution of cranial NC cells.

Malformation of the epibrachial placode was associated with fusion of branchial neural crest

Since a reciprocal interaction between NC and placodal cells is required for normal morphogenesis of these populations, we examined placode development in the *Xlphn2* morphant. The expression of the specific placode marker *Xfoxi4.1* (Schlosser and Ahrens, 2004) showed that the placodal cell population appeared normal at the neurula stage in the control MO and *Xlphn2* MO-injected embryos (Fig. 4 A,B). However, in the *Xlphn2* MO-injected tailbud-stage embryo, one of the epibranchial placode segment was disrupted (Fig. 4 C,D). qRT-PCR analysis of placode markers, *Xsix1* and *Xfoxi4.1*, showed that *Xlphn2* MO injection had no effect on *Xsix1* expression but slightly increased the expression of *Xfoxi4.1* (Fig. S4). These results reflected the broader expression pattern of *Xfox4.1* in the anterior epibranchial placodes of *Xlphn2* MO-injected embryo (Fig. 4D), and supported the conclusion that placodes were fused rather than lost. Double staining for NC cells and placodal cells indicated that the fusion of branchial arches was caused by loss of the epibranchial placode (Fig. 4 E-H). Thus, *Xlphn2* mRNA concentrated in the placode plays an important function in placode formation.

Xlphn2 is essential for neural crest migration in a non-cell-autonomous manner

To examine whether *Xlphn2* is required for the migration capability of NC cells or serves as environmental cue for NC cell migration, we performed transplantation experiments. First, we investigated the migration pattern of *tdTomato* (*tdTom*)-labeled NC cells excised from *tdTom*-injected embryos after transplantation into the control MO-injected embryos (Fig. 5 A-C, M). The transplanted *tdTom*-labeled NC cells migrated ventrally along the distinct streams in the control MO-injected embryos (17/22 embryos). By contrast, *tdTom*-labeled NC cells did not reach the branchial arches in *Xlphn2* MO-injected host (20/22 embryos) (Fig. 5 D-F, M). On the other hand, when we transplanted *tdTom*-labeled NC cells from embryos which were co-injected with *tdTom* mRNA and control MO or *Xlphn2* MO, were transplanted into the wild-type host, they migrated normally to the branchial arches (control MO 8/11, *Xlphn2* MO 9/12 embryos) (Fig. 5 G-L, M). These results suggested that *Xlphn2* was not required for the migration capacity of NC cells. Rather, these results demonstrate that *Xlphn2* is involved in the guidance of NC cells in a non-cell-autonomous fashion.

Discussion

Knockout of *Lphn2* in mice is embryonic lethal, implying fundamental functions of *Lphn2* in embryonic development. In this study, we found that *Xlphn2* is required for the proper migration and distribution of NC cells in the branchial arches. In the *Xlphn2* morphant, NC cells were localized abnormally and the third and fourth NC streams in the branchial arches were fused. *Xlphn2*-defective NC cells migrated in the normal embryos, while normal NC cells did not move in the *Xlphn2*-defective embryo. These results suggest that *Xlphn2* in the placode is important for the migration of NC cells. Branchial arches provide survival and environmental signals for differentiation of cranial cartilage when NC cells reach these regions (Szabo-Rogers *et al.*, 2010). NC cells in the *Xlphn2* morphant, which migrate slowly, may not receive sufficient survival signals during migration, leading to cranial cartilage defects. It is also possible that separation of third and fourth branchial arch NCs by placodes was required for normal growth of cartilage structure since branchial cartilage, which originated from them, was most severely affected in *Xlphn2* morphant.

Mayor and colleagues reported that placodes provide chemoattractant(s) and contact inhibition factor(s) for NC cells (Steventon *et al.*, 2014, Theveneau *et al.*, 2010, Theveneau *et al.*, 2013). These factors are essential for correct NC cell migration and segmentation of placodes. In agreement, ablation of NC cells abolished the formation of epibranchial structure (Theveneau *et al.*, 2010). Our NC cell transplantation data suggests that *Xlphn2* is required for the migration of NC cells as an environmental factor. Similarly, the Ephrin signaling pathway has been implicated in the guidance of NC cells. The dominant negative form of *EphA2* disrupts the separation of NC cells in the third and fourth arches (Helbling *et al.*, 1998). This phenotype is very similar to that of the *Xlphn2* MO-injected embryos. Since the expression level of *EphA2* was not changed in the *Xlphn2* MO-injected embryo (data not shown), *EphA2* is not considered a downstream regulator of Xlphn2.

Adhesion-class G protein-coupled receptors are important for cell-cell interactions and associations with the extracellular matrix (Langenhan *et al.*, 2013). *LPHN1-, 2-,* or *3*-expressing cells bind to cells expressing *Teneurin2* or *4* (Boucard *et al.*, 2014), indicating that latrophilin family proteins are involved in cell adhesion. We could not detect the expression of *Teneurin2* and *4* in NC cells or placodes during NC cell migration stages (data not shown). Therefore, there may be other ligand molecules for Xlphn2. The exploration of Xlphn2 binding protein(s) expressed in NC cells is critical for fully understanding the mechanism of action of Lphn2.

Materials and Methods

Embryos

Eggs were obtained by injecting human chorionic gonadotropin (Gestron: Denka Seiyaku, Japan) into female *Xenopus laevis*. Fertilized eggs were obtained by artificial insemination and dejellied using 2% L-cystein hydrochloride (WAKO, Osaka, Japan). Embryos were staged as described previously (Nieukoop and Faber 1956).

Molecular cloning of human and Xenopus *Lphn2*

Xlphn2 cDNA fragment was amplified by PCR using cDNA from stage 35 embryos as a template, and was cloned into pGEM-T vector. Primer sets for amplifying *Xlphn2* fragments were 5'-actagtgtataccctctgcc-3' and 5'-accagccaaatctgctccta-3'. Sequence was identical to the deposited

data for chromosome 4S. Human *LPHN2* cDNA was cloned by RT-PCR using cDNA of human monocytic leukemia cell line, THP-1 as a template. FLAG sequence was added to the C-terminal end of LPHN2 and cloned into pCS2⁺ vector.

RT-PCR

RT-PCR was performed as described previously (Tanegashima *et al.*, 2004). Total RNA was reverse-transcribed using PrimeScript RT reagent kits (Takara, Otsu, Japan). qRT-PCR was carried out using Thunderbird SYBR qPCR Mix (Toyobo, Osaka, Japan) and a LightCycler480 system (Roche Applied Science, Indianapolis, IN). Messenger RNA expression levels were determined using the relative quantification method (LightCycler480 software, Roche Applied Science) and *EF1a* as a reference gene. The primer sequences are listed in Table S1.

Microinjection

Two-cell *Xenopus* embryos were injected with 5 nl of capped RNA and/or MO in each of the animal blastomeres. The embryos were cultured in 0.1 X Steinberg's solution. MOs were synthesized by Gene Tools (Gene Tools LLC, Philomath, USA). The sequence of *Xlphn2* MO was 5'-CCTGCTGC-CAGGAGTCACCATTATT-3' (designed for translation initiation site). Gene Tool control MO (5'-CCTCTTACCTCAGTTACAATTTATA-3') was used as a negative control. Synthetic RNA was made using mMessage mMachine SP6 (Thermo Fisher, Waltham, USA). *Not*I-linearized pCS2⁺human *LPHN2-FLAG*, pCS2⁺*tdTomato,* pCS2⁺*EGFP*, and pCS2⁺*Xlphn2 5'UTR-EGFP* were used as templates. Injection experiments were done more than twice for phenotype analyses and WISH.

Alcian blue staining

Embryos were fixed overnight in 100% ethanol at stage 45, and stained with 0.01% Alcian blue (WAKO) in 20% acetic acid/EtOH for 3 days. After rehydration, samples were refixed in 4% paraformaldehyde (WAKO). Fixed embryos were treated with 2% KOH followed by several rinses to clear the cartilage structure. Head skin was removed to mount onto glass slides and photographed.

WISH

WISH was performed according to Harland (1991) using *Xlphn2*, *N-CAM*, *Xtwist*, *Xdlx-2*, and *Xfoxi4.1* as probes. pGEMT-*Xlphn2* was linearized by *Spe*I and transcribed by T7 polymerase to produce Digoxigenin (DIG)-UTP (Roche Applied Science, Penzberg, Germany)-labeled antisense probe, and by *Nco*I to produce sense probe. pBluescript-*N-CAM*, and *Xtwist* were linearized by *Eco*RI, pBluescript-*Xdlx-2* were linearized by *Spe*I. The linearized plasmids were transcribed by T7 polymerase (Takara, Otsu, Japan) to produce DIG-labeled antisense probe. pBluescript-*Xfox4.1.*, which was kindly provided by Dr. Sei Kuriyama (Akita University), was linearized by *Pst*I and transcribed by T3 polymerase (Takara) to produce DIG-labeled antisense probe. DIG-labled probes were detected by BM purple AP substrate (Roche Applied Science). For double staining, fluorescein-UTP (Roche Applied Science)-labeled *Xtwist* and DIG-labeled *Xfox4.1* probes were hybridized. The DIG-labeled probe was detected by BM purple AP substrate (purple) and the fluorescein-labeled probe was detected by 5-bromo-4-chloro-3'-indolyphosphate (BCIP, Roche Applied Sciences: light blue).

Transplantation

Control MO (40 ng) + *tdTom* mRNA (100 pg), X1*phn2* MO (40 ng) + *tdTom* mRNA (100 pg) or *tdTom* mRNA (100 pg) were used for microinjection at animal pole of 2-cell embryos. *tdTom*-labeled NC cells were dissected at stage 20, and transplanted to the right side of presumptive otic vesicle region of stage 20 embryo (wild-type, 40 ng Ctl MO-injected, or 40 ng *Xlphn2* MO-injected embryos). After fixation at stage 30, fluorescent imaging and morphology were photographed using a Leica M165 FC microscope (Leica, Wetzlar, Germany). Five independent experiments were carried out. The percentages of migrated NCs in different experiments are shown as means with standard error (Fig. 5M). Statistical analyses against

samples of control MO-injected host transplanted with *tdTom*-injected NC cells were performed using Fisher's exact t-test using the total number of transplanted embryos.

References

ANDERSON, G.R., MAXEINER, S., SANDO, R., TSETSENIS, T., MALENKA, R.C. and SUDHOF, T.C. (2017). Postsynaptic adhesion GPCR latrophilin-2 mediates target recognition in entorhinal-hippocampal synapse assembly. *J Cell Biol* 216: 3831-3846.

ARCOS-BURGOS, M., JAIN, M., ACOSTA, M.T., SHIVELY, S., STANESCU, H., WALLIS, D., DOMENE, S., VELEZ, J.I., KARKERA, J.D., BALOG, J. *et al.,* (2010). A common variant of the latrophilin 3 gene, LPHN3, confers susceptibility to ADHD and predicts effectiveness of stimulant medication. *Mol Psychiatry* 15: 1053-1066.

BOUCARD, A.A., MAXEINER, S. and SUDHOF, T.C. (2014). Latrophilins function as heterophilic cell-adhesion molecules by binding to teneurins: regulation by alternative splicing. *J Biol Chem* 289: 387-402.

CAPOGNA, M., VOLYNSKI, K.E., EMPTAGE, N.J. and USHKARYOV, Y.A. (2003). The alpha-latrotoxin mutant LTXN4C enhances spontaneous and evoked transmitter release in CA3 pyramidal neurons. *J Neurosci* 23: 4044-4053.

DEAK, F., LIU, X., KHVOTCHEV, M., LI, G., KAVALALI, E.T., SUGITA, S. and SUDHOF, T.C. (2009). Alpha-latrotoxin stimulates a novel pathway of Ca2+-dependent synaptic exocytosis independent of the classical synaptic fusion machinery. *J Neurosci* 29: 8639-8648.

HARLAND, R. M. (1991). *In situ* hybridization: an improved whole-mount method for *Xenopus* embryos. *Methods Cell Biol* 36: 685-695.

HELBLING, P.M., TRAN, C.T. and BRANDLI, A.W. (1998). Requirement for EphA receptor signaling in the segregation of *Xenopus* third and fourth arch neural crest cells. *Mech Dev* 78: 63-79.

HOPWOOD, N.D., PLUCK, A. and GURDON, J.B. (1989). A *Xenopus* mRNA related to *Drosophila* twist is expressed in response to induction in the mesoderm and the neural crest. *Cell* 59: 893-903.

HUANG, X. and SAINT-JEANNET, J.P. (2004). Induction of the neural crest and the opportunities of life on the edge. *Dev Biol* 275: 1-11.

KULESA, P.M., BAILEY, C.M., KASEMEIER-KULESA, J.C. and MCLENNAN, R. (2010). Cranial neural crest migration: new rules for an old road. *Dev Biol* 344: 543-554.

LANDER, R., NASR, T., OCHOA, S.D., NORDIN, K., PRASAD, M.S. and LABONNE, C. (2013). Interactions between Twist and other core epithelial-mesenchymal transition factors are controlled by GSK3-mediated phosphorylation. *Nat Commun* 4: 1542.

LANGENHAN, T., AUST, G. and HAMANN, J. (2013). Sticky signaling--adhesion class G protein-coupled receptors take the stage. *Sci Signal* 6: re3.

MARCUCIO, R., HALLGRIMSSON, B. and YOUNG, N.M. (2015). Facial Morphogenesis: Physical and Molecular Interactions Between the Brain and the Face. *Curr Top Dev Biol* 115: 299-320.

NIEUKOOP, P. D. and J. FABER. (1956). Normal Table of *Xenopus laevis* (Daudin). Elsevier North-Holland, Amsterdam, The Netherlands.

O'SULLIVAN, M.L., DE WIT, J., SAVAS, J.N., COMOLETTI, D., OTTO-HITT, S., YATES, J.R., 3RD and GHOSH, A. (2012). FLRT proteins are endogenous latrophilin ligands and regulate excitatory synapse development. *Neuron* 73: 903-910.

SZABO-ROGERS, H.L., SMITHERS, L.E., YAKOB, W. and LIU, K.J. (2010) New directions in craniofacial morphogenesis. *Dev Biol.* 341: 84-94.

SCHLOSSER, G. and AHRENS, K. (2004). Molecular anatomy of placode development in *Xenopus laevis. Dev Biol* 271: 439-466.

SCHLOSSER, G. (2006). Induction and specification of cranial placodes *Dev Biol* 294: 303-351.

SILVA, J.P., LELIANOVA, V.G., ERMOLYUK, Y.S., VYSOKOV, N., HITCHEN, P.G., BERNINGHAUSEN, O., RAHMAN, M.A., ZANGRANDI, A., FIDALGO, S., TONEVITSKY, A.G. *et al.,* (2011). Latrophilin 1 and its endogenous ligand Lasso/teneurin-2 form a high-affinity transsynaptic receptor pair with signaling capabilities. *Proc Natl Acad Sci USA* 108: 12113-12118.

SQUARE, T., JANDZIK, D., CATTELL, M., COE, A., DOHERTY, J. and MEDEIROS, D.M. (2015). A gene expression map of the larval *Xenopus laevis* head reveals developmental changes underlying the evolution of new skeletal elements. *Dev Biol* 397: 293-304.

STEVENTON, B., MAYOR, R. and STREIT, A. (2014). Neural crest and placode interaction during the development of the cranial sensory system. *Dev Biol* 389: 28-38.

TANEGASHIMA, K., HARAMOTO, Y., YOKOTA, C., TAKAHASHI, S. and ASASHIMA, M. (2004). Xantivin suppresses the activity of EGF-CFC genes to regulate nodal signaling. *Int J Dev Biol* 48: 275-283.

THEVENEAU, E., MARCHANT, L., KURIYAMA, S., GULL, M., MOEPPS, B., PARSONS, M. and MAYOR, R. (2010). Collective chemotaxis requires contact-dependent cell polarity. *Dev Cell* 19: 39-53.

THEVENEAU, E., STEVENTON, B., SCARPA, E., GARCIA, S., TREPAT, X., STREIT, A. and MAYOR, R. (2013). Chase-and-run between adjacent cell populations promotes directional collective migration. *Nat Cell Biol* 15: 763-772.

Further Related Reading, published previously in the *Int. J. Dev. Biol.*

Developmental expression of Pitx2c in Xenopus trigeminal and profundal placodes
Yeon-Ho Jeong, Byung-Keon Park, Jean-Pierre Saint-Jeannet and Young-Hoon Lee
Int. J. Dev. Biol. (2014) 58: 701-704
https://doi.org/10.1387/ijdb.140254js

Essential role of AWP1 in neural crest specification in Xenopus
Jeong-Han Seo, Dong-Seok Park, Mina Hong, Eun-Ju Chang and Sun-Cheol Choi
Int. J. Dev. Biol. (2013) 57: 829-836
https://doi.org/10.1387/ijdb.130109sc

Identification and gene expression of versican during early development of Xenopus
Paola Casini, Michela Ori, Angela Avenoso, Angela D'Ascola, Paola Traina, Walter Mattina, Roberto Perris, Giuseppe M. Campo, Alberto Calatroni, Irma Nardi and Salvatore Campo
Int. J. Dev. Biol. (2008) 52: 993-918
https://doi.org/10.1387/ijdb.082582pc

Msx1 and Msx2 have shared essential functions in neural crest but may be dispensable in epidermis and axis formation in Xenopus
Deepak Khadka, Ting Luo and Thomas D. Sargent
Int. J. Dev. Biol. (2006) 50: 499-502
https://doi.org/10.1387/ijdb.052115dk

Xerl, a novel CNS-specific secretory protein, establishes the boundary between neural plate and neural crest
S Kuriyama and T Kinoshita
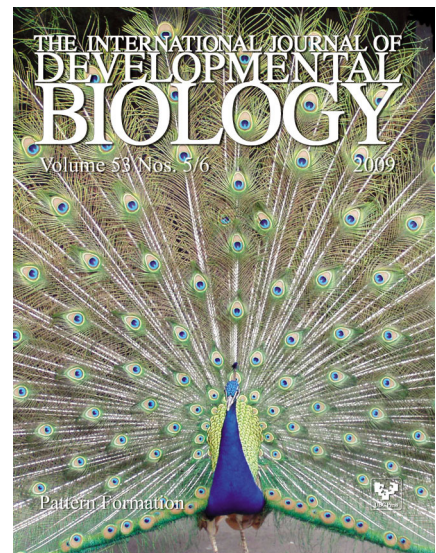Int. J. Dev. Biol. (2001) 45: 845-852
http://www.intjdevbiol.com/web/paper/11804027

The LIM homeodomain protein Lim-1 is widely expressed in neural, neural crest and mesoderm derivatives in vertebrate development
A A Karavanov, J P Saint-Jeannet, I Karavanova, M Taira and I B Dawid
Int. J. Dev. Biol. (1996) 40: 453-461
http://www.intjdevbiol.com/web/paper/8793615

Neural crest cell migration and pigment pattern formation in urodele amphibians
H H Epperlein, J Löfberg and L Olsson
Int. J. Dev. Biol. (1996) 40: 229-238
http://www.intjdevbiol.com/web/paper/8735933